Melting and phase transitions of nitrogen under high pressures and temperatures

Dane Tomasino, Zsolt Jenei, William Evans, and Choong-Shik Yoo

Citation: J. Chem. Phys. **140**, 244510 (2014); doi: 10.1063/1.4885724
View online: http://dx.doi.org/10.1063/1.4885724
View Table of Contents: http://aip.scitation.org/toc/jcp/140/24
Published by the American Institute of Physics

Melting and phase transitions of nitrogen under high pressures and temperatures

Dane Tomasino,[1] Zsolt Jenei,[2] William Evans,[2] and Choong-Shik Yoo[1]
[1]*Department of Chemistry and Institute for Shock Physics, Washington State University, Pullman, Washington 99164, USA*
[2]*Lawrence Livermore National Laboratory, Livermore, California 94550, USA*

(Received 22 April 2014; accepted 17 June 2014; published online 30 June 2014)

Dense nitrogen exhibits fascinating molecular and extended polymorphs as well as an anomalous melt maximum at high temperatures. However, the exact solid-liquid phase boundary is still the subject of debate, as both creating and probing hot dense nitrogen, solid and fluid alike, poses unique experimental challenges. Raman studies of nitrogen were performed to investigate the melting curve and solid-solid phase transitions in the pressure-temperature range of 25 to 103 GPa and 300 to 2000 K. The solid-liquid phase boundary has been probed with time-resolved Raman spectroscopy on ramp heated nitrogen in diamond anvil cell (DAC), showing a melting maximum at 73 GPa and 1690 K. The solid-solid phase boundaries have been measured with spatially resolved micro-confocal Raman spectroscopy on resistively heated DAC, probing the δ-ε phase line to 47 GPa and 914 K. At higher pressures the θ-phase was produced upon a repeated thermal heating of the ζ-phase, yet no evidence was found for the ι-phase. Hence, the present results signify the path dependence of dense nitrogen phases and provide new constraints for the phase diagram. © *2014 AIP Publishing LLC*. [http://dx.doi.org/10.1063/1.4885724]

I. INTRODUCTION

Simple molecular crystals at high pressure are characterized by strong intramolecular covalent bonds and weak intermolecular van der Waals interactions. The evolution of these systems under high pressures and temperatures is of fundamental scientific and technological importance[1] contributing to the field condensed matter physics and material sciences. Under sufficient compression, the nature of inter- and intramolecular interactions alters significantly and can give rise to new states of matter and interesting phenomena such as a melting maximum (the point on the solid liquid phase boundary at which $\partial T/\partial P = 0$ on a phase diagram). Often observed are the transformations of dense molecular species into ionic, metallic, and/or extended non-molecular phases.[2–4] However, the progression towards eventual electron delocalization and new chemical bonding is not always straight forward. As the molecular solids are compressed, they may undergo structural phase transitions with various types of orientational order such as those seen in CO_2 and H_2O.[5,6] Understanding the phase transitions and behavior of simple molecular systems over a wide P-T range and mapping the solid/solid and solid/liquid transitions is vital as they affect the energetic and kinetic barriers associated with transitions to extended structures.[7]

Nitrogen represents a classical diatomic system with a strong triple bond (N≡N) which is extremely stable at ambient conditions as well as under high pressures. For this reason nitrogen is considered to be a model system for understanding condensed matter theory of physical and chemical transformations.[8] Under modest compression nitrogen exhibits fascinating polymorphism with five solid molecular phases (α, β, γ, δ, ε) at pressures as high as 10 GPa and below 300 K. The low temperature phases of nitrogen are the orientationally disordered cubic α-phase[9] and ordered tetragonal γ-phase[10] which are controlled by quadrapole-quadrapole interactions. Upon isothermal compression at 300 K, fluid N_2 solidifies into the disordered hexagonal β-phase at 2.4 GPa,[11] and into the cubic δ-phase at 4.9 GPa,[12] which exhibits both spherical and disk-like orientational disorder. Further compression reveals a distortion of the cubic lattice at 10.5 GPa to that of the tetragonal δ^*-phase[13] followed by the orientationally ordered rhombohedral ε-phase[14] at 16.3 GPa, and the ζ-phase[15,16] at 60 GPa with proposed orthorhombic structure. These solid nitrogen phases have been studied extensively over a wide P-T range,[9–18] however the δ-ε phase boundary is not well known at high pressures and temperatures. Recent experimental work has lead to the discovery of two new phases of molecular nitrogen, ι and θ-phases.[19] The phase boundaries and formation of the latter two phases are, however, not well understood as they are only accessible at high pressures and temperatures.

The melt line of nitrogen is well defined in the low pressure region from 0–18 GPa up to 897 K.[20] Above this range the melt curve is the subject of some debate. The nitrogen melt curve has gained significant attention as first-principles theoretical calculations[21] predict a melting curve maximum and a first-order liquid-liquid phase transition, similar to those found in its periodic analog phosphorous.[22,23] Recent calculations suggested that nitrogen may also transform from a molecular liquid to a polymeric fluid.[24] Two experimental studies have probed the melt curve to higher pressures and temperatures (up to 120 GPa and 2500 K),[25,26] however the results of these studies largely disagree, likely stemming from differences in the methods to probe the onset of melting and

the determination of temperature. Hence, the purpose of this report is threefold: (i) to resolve the longstanding dispute of the high P-T melting curve and the possibility of a melting curve maximum and existence of a first order liquid-liquid phase transition, (ii) to probe the solid-solid transitions of the δ-ε-ζ-phases at high temperatures and investigate the existence and phase range of the ι and θ-phases, and (iii) to understand the path-dependent transformations of dense nitrogen phases.

II. EXPERIMENTAL METHODS

Investigating nitrogen at high pressures and temperatures creates unique experimental challenges from the high mass and thermal diffusivities. In order to probe the region of interest, greater than 20 GPa with temperatures exceeding 2000 K, two experimental methods were employed. First, the melt curve was determined using laser heated diamond anvil cell (DAC) techniques[27] and Raman spectroscopy. In the pressure range of interest nitrogen is optically transparent and will not readily absorb radiation from the heating laser. Thus an indirect heating method was employed using a tantalum toroid as a thermal absorber which is easily heated by available laser radiation sources.[28] The average dimensions of the metal absorber were ≈60 μm in diameter and 5 μm thick with the central aperture ≈8 μm in diameter as seen in Figure 1(a). Heating was performed using a single sided 1070 nm 100 W ytterbium fiber laser operating in a controlled trapezoidal pulse mode with pulse lengths averaging 75 s allowing for a slow continuous temperature increase and decrease (Fig. 2 inset). The near-IR laser was defocused to approximately 50 μm in diameter produce a uniform heating of the toroid. Figure 1(b) shows the uniform heating of metal absorber. The hot nitrogen contained within the central aperture was probed with a confocal time-resolved Raman spectroscopy in a backscattering geometry[29] using a high powered 532 nm laser and a gated and intensified CCD detector. The Raman probe laser spot size was focused to ≈5 μm in diameter to fit inside the toroid aperture. In general 50 spectra were taken with 1 s exposure per spectrum during the heating/cooling cycle. Pressure was determined through ruby luminescence[30] and confirmed with the high frequency edge of the diamond phonon[31] and the calibrated nitrogen vibrational frequency. Pressure measurements were made before and after the heating cycle and did not vary more than ±1 GPa. The thermal pressure of the sample during heating is unknown and is estimated to be less than 10%.[32]

Temperature measurements were made by collecting the thermal radiation from the absorber in the area just a few microns around the central aperture and fitting it to the Planck

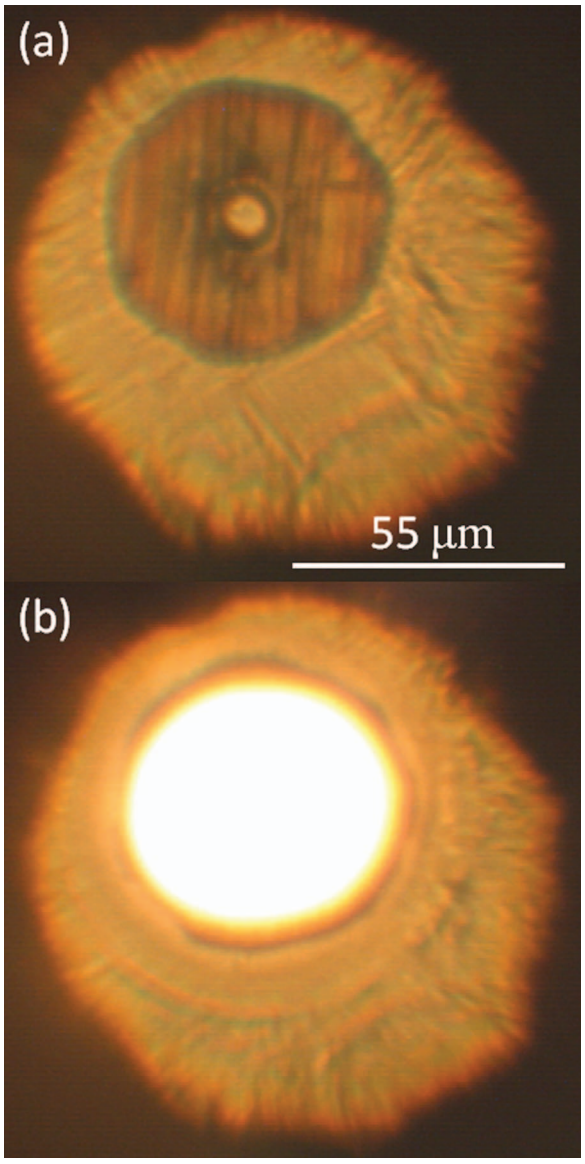

FIG. 1. (a) The sample chamber of the DAC at 49 GPa before laser heating. The metal absorber used to heat the sample is approximately 60 μm wide and 5 μm thick with an inner diameter of approximately 8 μm. (b) The glowing metal absorber during the heating process. Liquid nitrogen can be seen extending out from the outer edge of the absorber. Light just outside the center sample cavity was used to determine temperature through spectral radiometry.

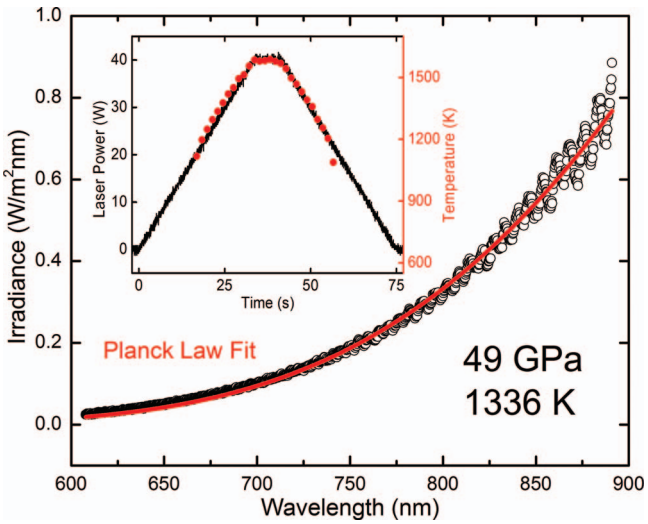

FIG. 2. Fitting of the spectral irradiance taken at 49 GPa with the Planck's gray body radiation equation to determine temperature of the laser heated sample. Inset shows the trapezoidal laser pulse profile used to heat the sample, the synchronized time-resolved temperature measurements that follow the pulse profile.

radiation function using emissivity and temperature as free fitting parameters.[33] A gray body approximation was invoked whereby the emissivity of the absorber was held constant as a function of both wavelength and temperature. It has been shown that the error associated with this approximation is quite low when fitting irradiance in the spectral regions below 1000 nm.[34] However at the highest temperatures, greater than 1500 K, error may be on the order of 100 K due to the unknown emissivity wavelength dependence.[35] The thermal spectrum was collected in a time resolved manner and synchronized to collect light in the middle of the Raman collection period with an average exposure of 10 ms. Shown in Fig. 2 is a typical example of the fitting of the collected thermal radiation under ramp heating just below the melt line of nitrogen with statistical error of ±3 K. Spectrum collected at higher temperatures above the melt line often had slightly nosier spectrum with a less accurate fitting with a fitting error on the order of ±10 K. The cause of this is the thermal expansion of the sample chamber and the DAC at extreme temperatures (usually greater than 1500 K). The focal distance of the sample is slightly perturbed causing the slightly noisier spectrum. The fitting of the time-resolved thermal radiation spectra was treated consistently across the entire temperature range to determine the most accurate data. As evident in the Fig. 2 inset, the continuity of the fitting process determined temperatures that closely follow the ramp laser power profile.

Additional sources of error in the determination of temperature of the hot dense nitrogen may come from radial or axial temperature gradients in which the sample is colder than the metal absorber. In theory, a material with low thermal conductivity would suffer from radial temperature gradients the farther the sample is from the heat source, and the high thermal conductivity of the diamonds would produce an axial temperature gradient as well. This of course is largely dependent on the particular setup of the sample chamber. Current experimental techniques do not allow for the authors to determine the temperature gradients (both radial and axial) within the small central aperture of the metal toroid cavity as the inner sample cavity is far too small, and the sample chamber much too thin (not more than 10 μm thick). Fluid nitrogen phase is mobile, which will reduce the possible temperature gradients. As can be seen in Fig. 1(b) fluid nitrogen can be seen extending considerably beyond the outer diameter of the metal absorber. There may be a temperature gradient within the sample cavity, but we propose that it will be small given circular uniform heating from the particular size and shape of the metal absorber (which was never more than 10 μm in diameter), and the light convecting nature of the nitrogen sample. Thus, by probing exclusively the nitrogen contained within the small center cavity of the metal toroid the temperature error is expected to be well within the error of the Raman determination of the phase transition.

Maintaining and measuring temperatures below 800 K with laser heating and optical pyrometry are quite challenging due to the high thermal conductivity of diamonds and relatively low thermal emission of metal absorbers. Therefore, to investigate the lower temperature solid phases (300–1000 K), a second method was used to externally (or ohmically) heat the DAC. He-gas driven membrane DAC was adapted to maintain long-term thermal and mechanical stabilities and small pressure/temperature gradients at high temperatures. This was accomplished by performing the heating experiments in a vacuum chamber to prevent oxidation of the cell and graphitization of the diamond. Dual internal micro heaters were built to heat the sample while minimizing possible temperature gradients with temperature measured by thermocouples in contact with both diamonds.[36] The mechanical stability of the sample chamber was improved by the use of W-Re gaskets which held constant pressures at temperatures in excess of 900 K. Pressure was measured through ruby luminescence,[30] and corrected for temperature at high T to determine the most accurate pressure possible.[37] At temperatures higher than 500 K we measured the shift of the ^7D-^5F fluorescence line of the SrB_4O_7:Sm^{2+} compound for *in situ* pressure determination. The shift in the fluorescence line with pressure has been calibrated by Datchi *et al.*,[38] and unlike ruby does not require temperature correction. It is difficult to maintain constant pressure in isobaric experiments during heating due to slight thermal pressure. To counter this temperature increase was slow thus maintaining constant pressure was achieved through the manipulation of the gas pressure of the membrane DAC. The vacuum vessel was outfitted with glass windows to allow for visual and spectroscopic analysis of the sample during heating.

III. RESULTS AND DISCUSSION

A. Laser heating and the melting curve

The melting curve was probed from 20 to 89 GPa utilizing the laser heating method described above. In this pressure range melting was determined *in situ* (Fig. 3) through changes

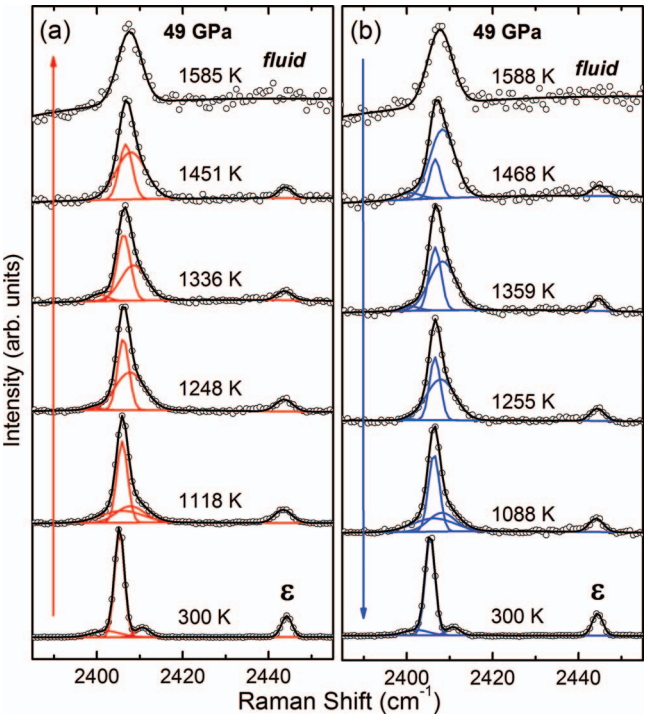

FIG. 3. (a) The heating and (b) cooling cycle of ε-phase nitrogen at 49 GPa as it is driven from 300 K into the fluid phase and back to 300 K. The solid nitrogen remains as ε-phase as it is heated and cooled.

in the vibrational spectrum. Raman scattering was collected in both the heating (Fig. 3(a)) and cooling (Fig. 3(b)) cycle as shown. At 49 GPa and 300 K the solid nitrogen is in the ε-phase with four clearly resolvable characteristic Raman frequencies at 2399.6 cm^{-1} $\nu_{2c(2c)}$, 2405.1 cm^{-1} $\nu_{2c(2a)}$, 2410.6 cm^{-1} ν_{2b}, and 2444.2 cm^{-1} ν_1.[39] The peak splitting seen in nitrogen is caused by nitrogen molecules occupying different site symmetries in the rhombohedra lattice. As the sample is heated the ν_2 vibrons slightly blue shift and broaden while the ν_1 vibron slightly red shifts and becomes broader as well. These peaks (deconvoluted) are visible to high temperatures just below melt as seen in the strong asymmetry of the ν_2 vibron at 1451 K in the heating cycle (Fig. 3(a)). A transformation to the partially orientationally disordered δ-phase would be indicated by the loss of the splitting of the ν_2 as only a single ν_1 and ν_2 are present in this phase which correspond to the molecule occupation of sites with sphere and disk like disorder. Our results indicate that nitrogen entered the fluid state from the solid ε-phase as ν_2 splitting can be seen before entering the melt. In the fluid state the distinction of site symmetry is lost, as nitrogen is completely disordered. Thus, this was taken as the evidence of melting. The melting point was then chosen to be in between the lowest temperature where a solid is still visible just before melting and the highest temperature where the liquid is visible from both the heating and cooling cycles (Fig. 4) as seen in the vertical error bars. Upon cooling from the melt, nitrogen regains the ν_1-ν_2 vibrational splitting in the Raman spectra as the molecules lock into lattice positions. As seen in Fig. 3(b), the cooling at 49 GPa demonstrates the return of the ε-phase nitrogen with peak positions at 300 K recorded at 2399.6 cm^{-1} $\nu_{2c(2c)}$, 2405.8 cm^{-1} $\nu_{2c(2a)}$, 2410.6 cm^{-1} ν_{2b}, and 2444.2 cm^{-1} ν_1. Thus, indicating ε-δ solid structural transition was not observed as the solid nitrogen is heated into, or cooled from the liquid phase. The peak shifts, disappearance and return of the ν_1 vibron seen in Fig. 3 at 49 GPa is typical of the changes seen throughout the pressure region studied with laser heating. The δ-ε transition occurs at 16.3 GPa at room temperature, however the changes in both the low and high frequency Raman modes from the slow rhombohedral distortion are subtle, especially with increased thermal broadening. Detecting the ε-δ at pressures at pressures lower than 45 GPa is difficult due to the small differences in the Raman spectra where changes in the vibrational spectrum are not easily resolvable. Therefore, no solid-solid transitions were observed with laser heated samples, however, the disappearance of site symmetry was clearly visible through the pressure range studied to unambiguously determine melting. The error bars in Fig. 4 are a product of the error in determining the solid-liquid phase change from the melting and solidification indentified in the Raman spectra, not from error in the temperature determination which is presumably smaller.

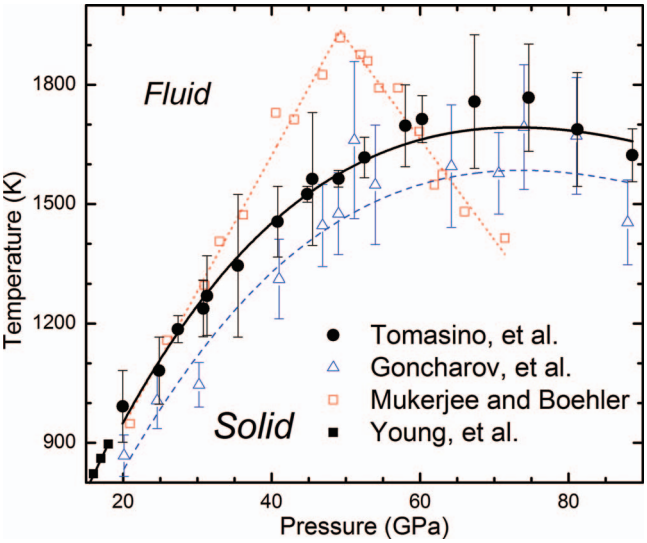

FIG. 4. The phase diagram of N_2 in the region of melting. Solid black circles are from the present study, and the black solid line fit to the Kechin equation. Solid black squares from Ref. 19, open red squares from Ref. 24, and open blue triangles from Ref. 25 also fit to the Kechin equation (the dashed blue line). The inset shows sample with a metal toroid absorber used in laser-heated studies at 49 GPa.

The melt curve from this study represented in the high temperature phase diagram of Fig. 4 has been fit to the Kechin equation,[40] $T_m = T_0(1 + \Delta P/a)^b \exp(-c\Delta P)$, (a thermodynamic equation of state that allows for a maximum in the melt curve) with ambient pressure melting temperature $T_0 = 63.2$ K from Ref. 20. The proposed melt curve is in strong agreement with the existing low temperature melt line[20] and at higher pressures exhibits a broad melting maximum at 73 GPa and 1690 K. This melting maximum thus implies that the liquid has become denser than the underlying solid giving rise to a volume reduction as nitrogen enters the liquid state. The origin of the downturn in the melting maximum can be interpreted in several ways. A structural phase transition in the solid, such as the δ-ε transition, may be the source of the broad downturn. This is unlikely however as no change in the crystal structure of solid nitrogen was observed above 49 GPa at any temperature and the density differences between the two phases at high pressure are small, likely having little impact on the slope of the melt curve. This downturn may also be interpreted as a transition in the liquid from a molecular liquid to a polymeric fluid as predicted by Donadio *et al.*[41] to take place at ≈88 GPa and 2000 K and whose theoretically proposed high pressure melt curve slope agrees very well with the current study. However, at the maximum temperature probed in this study, 2178 K at 75 GPa, nitrogen still exhibits a strong molecular vibration in the fluid state without an evidence of N = N and/or N–N vibrational peaks associated with the polymeric fluid. Even at 89 GPa and 1733 K the nitrogen Raman spectra are distinctively in the frequency range of N≡N triple bond vibrations. Thus, the present study found no evidence of a first-order liquid-liquid transition in the vicinity of the melting maximum. Nevertheless, it is entirely possible that the high pressure liquid is a two or more component system that includes molecular and polymeric fluids of nitrogen allotropes with smoothly varying composition across the melting maximum. As such, the changes in the fluid nitrogen beyond the maximum and just above the melt line may be too subtle to resolve with current experimental techniques.

In comparison to the previously reported melt curves,[20,25,26] the present melting data are different in

both temperature and pressure for most of the melt range. Reference 25 reported a linear extension of Ref. 20 and a sharp melting maximum at 50 GPa and 1920 K, and subsequent linear decrease in the melt line as seen in Fig. 4. Our data are in good agreement with Ref. 20, extrapolated below 20 GPa, and Ref. 25 to approximately 30 GPa. Beyond this range the melt line and that of Ref. 25 diverge with our data being lower in temperature and exhibiting a slight curvature and slow turnover in the melt curve giving a broad melting maximum. The differences between our data and that of Ref. 25 are likely due to the different methods used to determine the onset of melting. Whereas the current study employed Raman spectroscopy, Ref. 25 utilized visual observations from laser speckle motion exclusively to determine the melting transition, with temperature determined from optical pyrometry in both studies. It has been noted that strong recrystallization effects from temperature cycling and a large increase in the viscosity of the liquid at high pressures decrease the certainty in movement of the laser interference pattern, thereby, creating substantial difficulties in determining the onset of melt.[25] Raman spectroscopy, by comparison, directly probes the vibrational signature of a system, which is extremely sensitive to its environment and the nature of bonding. Observing changes in the vibrational spectrum allows for a more accurate determination of the solid-liquid phase transition.

In contrast, the melt data reported from Ref. 26 (which we also fit to the Kechin equation[38]) were determined by Raman spectroscopy and follow a similar curvature to our data with a maximum at 73 GPa and 1585 K. The obvious difference is the reported temperature of melting being ≈120 K below our data throughout the pressure range studied. Extrapolating the melt line of Ref. 26 to pressures below 20 GPa reveals a phase line significantly below that of Refs. 20, 25, and the current work. The similarity in the melt line curvature suggests that it is the method of determining temperature that accounts for the discrepancy. Temperature from Ref. 26 was determined through Stokes/anti-Stokes intensity ratio of the peaks of the molecular vibron and sidebands from thermally excited states. In principle, this should yield accurate temperatures by probing an intrinsic property of the material. However, extrapolating the low pressure region of the melt curve below 20 GPa shows that Ref. 26 is substantially lower than the well defined phase line from Ref. 20. There are multiple challenges associated with using Stokes/anti-Stokes intensity ratios for the determination of temperature. The fundamental vibrational frequency of nitrogen is ≈2400 cm^{-1} under high pressures. The Boltzmann distribution of the first excited state of these higher energy vibrations is quite low, thus only at higher temperatures can one make an accurate determination of the temperature. Moreover, it is necessary to integrate over all vibrational and lattice modes to determine temperature accurately which can become very difficult at high temperatures, caused by the inevitable contribution of thermal radiation to the spectra at high T and the extremely weak and broad librons. Also inherent is the non-linear response of modern spectrograph diffraction gratings and CCD detectors. Large spectral regions (in the case of nitrogen ≈4800 cm^{-1}) will have a much larger discrepancy in the quantum efficiency of the diffraction grating and CCD in comparison to lower frequency vibrations. Temperature measurements made using this method from vibrational frequencies greater than 1000 cm^{-1} are inherently less accurate[42] than those determined from low frequency vibrations, possibly giving lower values. For this reason the method of fitting thermal emission to a Plank blackbody curve may be more accurate, especially with a small central toroid aperture and thin sample chamber to reduce possible temperature gradients, which should be small for dense convecting liquids. Comparing the current proposed melt line, which is similar to that of Ref. 26, to previous experimental studies[20,25,26] the longstanding dispute of the high pressure melt curve has been resolved. The current data provide the most accurate P-T constraints on the melt line with the melt line exhibiting a broad maximum at 73 GPa and 1690 K.

B. External heating and solid transformations

Solid nitrogen was probed from 20 to 102 GPa at temperatures ranging from 300 to 925 K using the external heating method described above. Raman scattering experiments were performed both in isothermal compression (Fig. 5(a)) and isobaric heating (Fig. 5(b)) to probe the solid phase boundaries at high pressures and temperatures. The δ-ε phase transition can be seen in Fig. 5(a). At 32 GPa and 690 K the δ-N_2 is identified by two peaks seen at ≈2400 cm^{-1}, which correspond to the sphere and disk-like orientation of the molecules occupying different symmetries.[12] This disordered phase does not exhibit defined lattice modes as seen at the low frequency range. As pressure is increased to 42 GPa δ-N_2 converts into orientationally ordered rhombohedral ε-phase. The ε-phase can be identified by the appearance of the low frequency

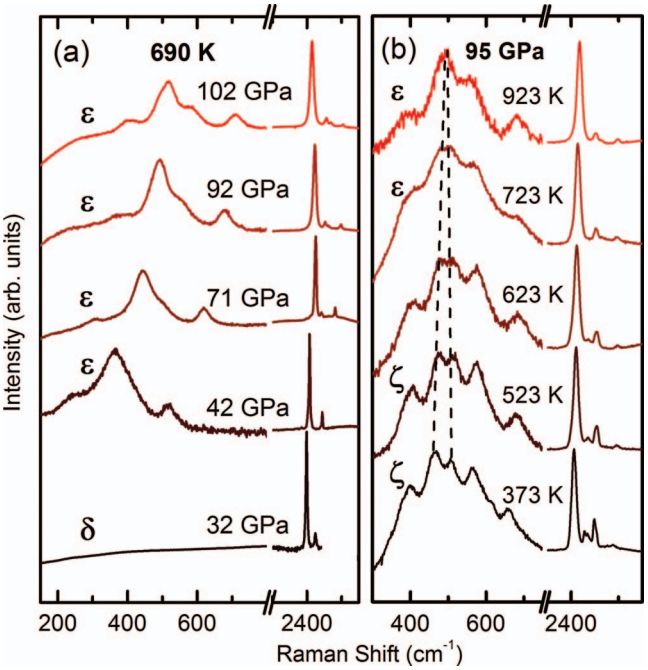

FIG. 5. (a) The isothermal compression of nitrogen at 690 K from 32 to 102 GPa showing the δ to ε-phase transition. (b) The isobaric heating at 95 GPa from 373 to 923 K showing the ζ to ε-phase transition.

lattice modes and further splitting of the vibrons as the symmetry of the cell is reduced. The high frequency changes at the onset of the transition are subtle as the volume changes are small[18] but can be seen as pressure is further increased and the ν_1 and ν_2 vibron branches split as a result of further distortion of the unit cell. As seen in Fig. 5(a), the ε-phase was compressed to 102 GPa at 690 K without any further observed structural transitions.

The isobaric heating of nitrogen at high pressures was utilized to reveal the transition from ζ to ε-phase, Fig. 5(b). Upon compression at room temperature the ε-phase transforms into ζ-phase at ≈60 GPa. The proposed orthorhombic structure of ζ-N_2[15,16,18,19] is a structural transition with a lowering of the site symmetry. In the Raman spectra this can be observed as an increase in the number of lattice bands, and further splitting of the ν_2 vibron as molecules move onto different sites. The characteristic low frequency Raman features of ζ-N_2 are very broad and the internal vibrations are difficult to resolve at ambient and high temperatures. At 95 GPa and 373 K (Fig. 5(b)) ζ-N_2 shows six lattice modes at 400.6, 469.0, 505.9, 566.6, 612.9, and 654.8 cm^{-1} and four vibrons at 2406.1, 2428.6, 2448.8, and 2486.7 cm^{-1}. As the sample is heated at 95 GPa, changes in both the low and high frequency Raman bands can be observed as ζ-phase transforms to ε-phase. By 923 K only four lattice modes can be observed at 397.7, 498.8, 555.3, and 679.8 cm^{-1} and three vibrons at 2417.4, 2452.1, and 4499.0 cm^{-1} (Fig. 5(b)) are observed, indicating the sample is clearly in the ε phase.

It has been reported that two additional polymorphs of molecular nitrogen exist, ι- and θ-phases, at high pressures and elevated temperatures.[19] The higher pressure phase, θ, was first discovered by pressurizing N_2 isothermally at 300 K above 95 GPa and then heating to temperatures greater than 600 K. In our study θ-N_2 was not accessible through this thermodynamic pathway (Fig. 5(b)). Instead, it was observed that upon quenching the sample from high temperatures at high pressures the Raman spectra changed slightly, showing signs of possible lattice strain or subtle structural distortions. This can be seen at the bottom of Fig. 6(a) in which the "fresh" nitrogen, and nitrogen that has been "quenched" from high temperatures at 75 GPa are compared at room temperature. In the low frequency range the Raman modes have the same number of peaks, but exhibit changes in intensity and frequency. This quenched sample is heated along the 75 GPa isobar to 920 K, then subsequently isothermally compressed to 102 GPa at 920 K. At 97 GPa the sample is completely transformed to θ-phase evidenced by the dramatic change in the vibron frequency and complete orientational ordering seen in the sharp low frequency lattice modes, both of which differ from all other known molecular phases.[19] The path dependence is made evident by comparing spectra at the same high P-T conditions as seen in Fig. 6(b), "fresh" and previously temperature "quenched" nitrogen which results in two very different structures.

A summary of our findings is presented on the high P-T solid phase diagram (Fig. 7) plotted alongside previous experimental work. Our current data are not in complete agreement with the existing phase diagram, especially with regards to the position of the δ-ε phase boundary. The established phase

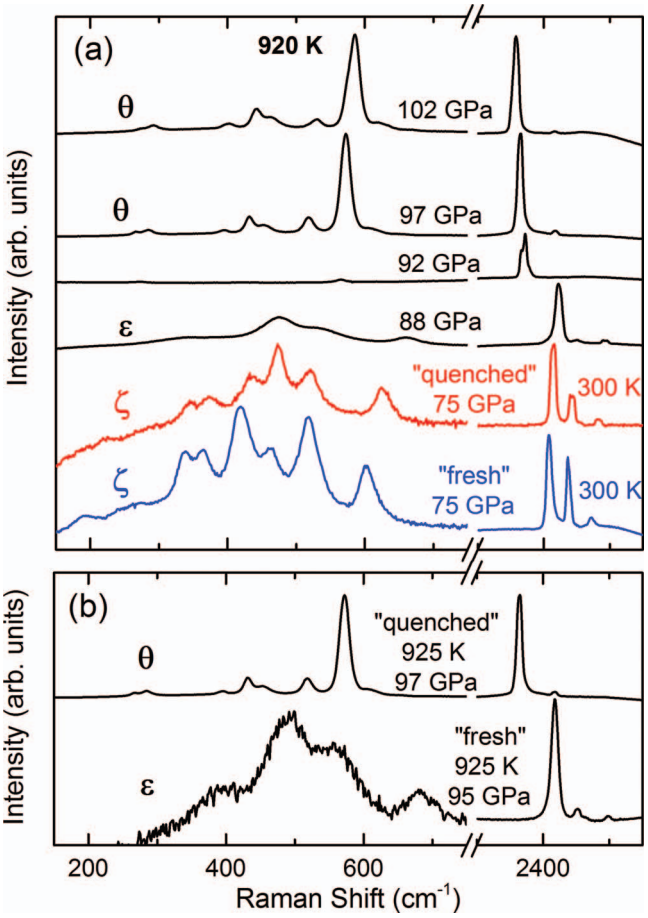

FIG. 6. (a) The path dependence of the θ-phase is displayed showing the differences of "fresh" and previously temperature "quenched" ζ-phase. Sample was subsequently isobarically heated at 75 GPa to 920 K then isothermally compressed to 102 GPa. (b) Displaying the different phases of "fresh" and "quenched" nitrogen at the same P-T conditions.

boundary from Refs. 15, 18, and 19 matches well with our data to 27 GPa and 480 K. Above this range our data take on a slight curvature and are pushed upwards. Extrapolating this phase line to the melt curve connects the δ-ε phase boundary near the melting curve maximum. The δ-ε transition reported by Ref. 26 was probed using laser heating, with the transition seemingly determined by the appearance of new vibrons in the vicinity of the ε-phase ν_1 and ν_2 peaks, assigned as belonging to the δ-phase, or perhaps the disappearance of the sharp low frequency ε-phase lattice modes. This may be the result of probing both hot and cold ε-phase, caused by large temperature gradients across the sample. For this reason the externally heated sample provides a more reliable method for probing phase transitions at temperatures substantially below the melt. This transition may also be confused for the appearance of ι-phase which was also reported in Ref. 26. Our reported phase boundary between ζ and ε did not dramatically deviate from that of Ref. 19. Our transition is slightly higher which may be explained by the difficulty in observing the subtle changes between ζ and ε-phases.

Interestingly, not observed in the present study is the formation of the ι-phase despite a rather extensive search over a wide range of pressures, temperatures, and thermal paths. This includes the entire P-T range studied as well as

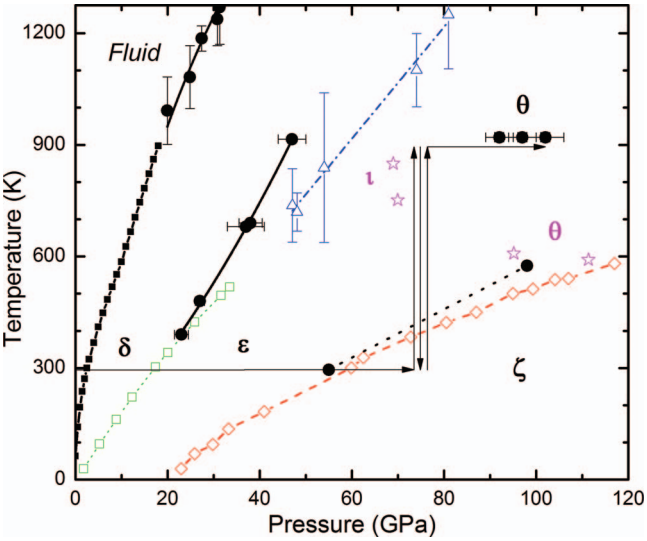

FIG. 7. The phase diagram of N_2 in the solid phase. Solid black circles are from current study. Solid black squares from Ref. 19, open green squares and open red diamonds from Refs. 17 and 18, open blue triangles from Ref. 25, open purple stars with ι and θ symbols from Ref. 18. Black arrows show the path P/T pathway used to produce path-dependant θ-phase in the current study.

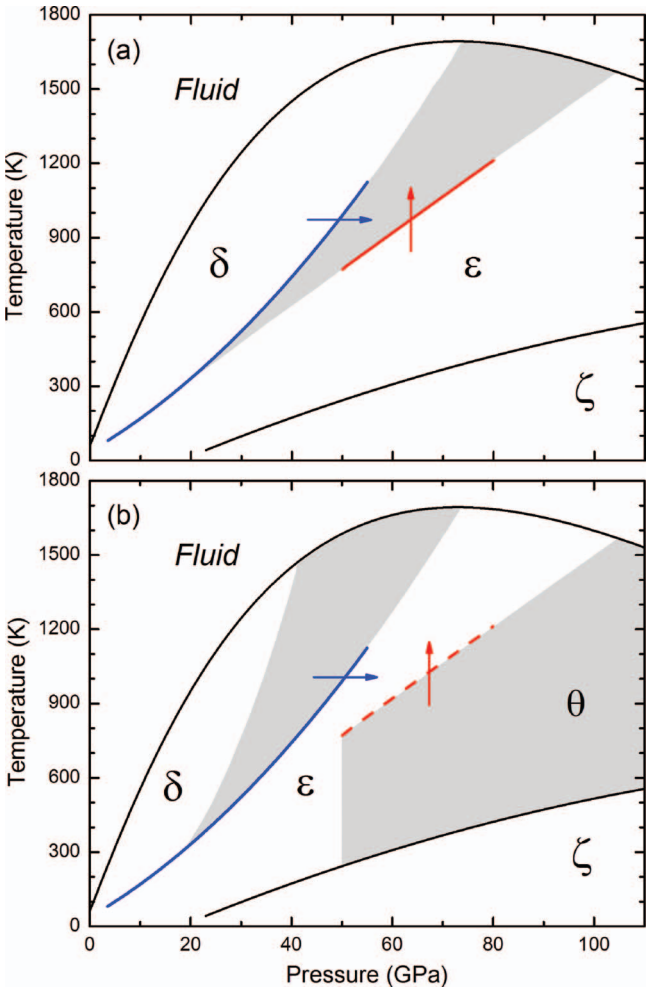

FIG. 8. (a) A conceptual phase diagram highlighting the discrepancy of the δ-ε phase transition (gray area) between our data and pathway to formation (blue line and arrow) and that of Ref. 25 (red line and arrow). (b) A conceptual phase diagram showing a corrected δ-ε phase transition region and the region of complex structural transitions (gray area) with strong path dependence.

where it was reported to be produced at pressures as low as 48 GPa[26] from laser heating, and 65 GPa[19] using external heating methods. As seen in Fig. 3, ι-phase was not formed by laser heating ε-phase nitrogen at 49 GPa into the melt and cooling to room temperature. Laser heating the same "quenched' sample at the same and elevated pressures did not convert the ε-phase to ι-phase. We conjecture that formation of ι-N_2 may be strongly influenced by the rate of heating/cooling which was on average $\pm$50 K/s in our experiments, or perhaps thermal path dependence, especially when quenching from the melt phase. We were also unable to produce the ι-phase through the isothermal compression as exemplified in Fig. 5(a) at 690 K. This illustrates that the ι-phase may have strong path dependence much like the θ-phase, which is only assessable from a previously temperature quenched sample of a distorted ζ-phase. This underscores the importance of further study on solid nitrogen as its accessible molecular phases exhibit strong kinetic and thermodynamic dependence. The open question remains as to what is the stability field of the stable (or perhaps metastable) high pressure and temperature molecular phases, and what is the kinetic/thermodynamic pathway to capture ι-phase and other yet to be discovered phases.

IV. SUMMARY

Based on the present and previous studies,[15,18,19,25,26] we propose a conceptual phase diagram (Fig. 8), providing new constraints for the melting curve and the solid-solid phase boundaries at high pressures and temperatures. Figure 8(a) highlights the current δ-ε phase line (blue line) and thermodynamic pathway used to determine it in a blue arrow. The blue line represents the combination of our data and that of Ref. 18 which was simply fit to a least squares refinement. Following that fitting up to the melt curve gives the lower pressure edge of δ-ε transition in Fig. 8(a). The high pressure edge (red line) of Fig. 8(a) is from the linear extrapolation of the ε-δ phase transition reported in Ref. 26 with a red arrow indicating the corresponding P-T pathway. The gray region in between thus represents the region of dispute up to the melting line. This representation, however, seems to violate what has been understood, and at present observed, about the kinetics and thermal path dependence of the transitions between dense solid phases. That is, an enhanced stability region observed for the parent phase resulting from strong interactions of dense molecules and thereby a large pressure (or temperature) hysteresis in the transition. As such, in the case of nitrogen the isothermal compression (blue) would push the δ-ε transition to a higher pressure than the isobaric heating (red), whereas the isobaric heating would drive the transition to be seen at a higher temperature and lower pressures than the isothermal compression. This is exactly opposite to what is shown in Fig. 8(a). Nevertheless, this chemical concept of the phase transition may explain why the δ-ε transition was not observed in our ramp laser-heating experiments at 49 GPa.

Figure 8(b) illustrates the phase diagram which represents a more accurate depiction of the phase transitions under the melt curve. The gray region of uncertainty has been shifted to lower pressures in accordance to our observations seeing only the ε-phase under the laser heating at 49 GPa. In the gray area below the red dashed line extrapolated to the melt curve signifies the complex region wherein strong kinetic and thermodynamic path dependence determine the structural distortion and transformation and thereby a specific "phase" to be observed. This is exemplified by the formation of θ-phase, only observed from previously temperature-quenched samples, and the lack of evidence for the formation of ι-nitrogen. In turn, the gray area signifies the P-T domain where the transition of nitrogen is strongly governed by kinetics and structural distortions.

In conclusion, the present study resolves the location of the high P-T melt curve and confirms the existence of a melting maximum at 73 GPa and 1690 K. The existence of a first-order liquid-liquid phase transition in the vicinity of the melt maximum was not observed, however the transition may consist of a two component system leading to a broad turnover in the melting curve. The phase diagram at temperatures below the melt curve was explored and an extension of the δ-ε transition was proposed which lies at considerably higher temperatures than previously reported.[26] We were unable to obtain the new molecular ι-phase in the phase space in which it was reported[19] possibly due to strong path dependence. The θ phase was produced at pressures near 100 GPa and exhibited strong path dependence as it was only assessable through the heating of a previously temperature quenched ζ-phase. An important general conclusion of this study is that a definitive determination of the equilibrium phase relations of strongly interacting nitrogen molecules is quite complex due to the transformational barriers of different structures within the same phase space. The reported results highlight the need for continued study to better understand the behavior of simple molecules under high compression and elevated temperatures, the stability and metastability of phases, and the thermodynamic and kinetic barriers associated with their formation.

ACKNOWLEDGMENTS

The present study at WSU has been supported by NSF-DMR (Grant No. 1203834) and DTRA (HDTRA1-12-01-0020). The work at LLNL was performed under the auspices of the U.S. Department of Energy under Contract No. DE-AC52-07NA27344.

[1]J. S. Schilling, J. Phys. Chem. Solids **59**, 553 (1998).
[2]V. Iota, J.-H. Park, and C. S. Yoo, Phys. Rev. B **69**, 064106 (2004).
[3]R. P. Dias, C. S. Yoo, M. Kim, and J. S. Tse, Phys. Rev. B **84**, 144104 (2011).
[4]V. Iota, C. S. Yoo, and H. Cynn, Science **283**, 1510 (1999).
[5]J. H. Park, C. S. Yoo, V. Iota, H. Cynn, M. F. Nicol, and T. Le Bihan, Phys. Rev. B **68**, 014107 (2003).
[6]C. G. Salzmann, P. G. Radaelli, B. Slater, and J. L. Finney, Phys. Chem. Chem. Phys. **13**, 18468 (2011).
[7]C. S. Yoo, M. Kim, W. Morgenroth, and P. Leirmann, Phys. Rev. B **87**, 214103 (2013).
[8]R. J. Hemley, Annu. Rev. Phys. Chem. **51**, 763 (2000).
[9]J. A. Venables and C. A. English, Acta Crystallogr., Sect. B **30**, 929 (1974).
[10]R. L. Mills and A. F. Schuch, Phys. Rev. Lett. **23**, 1154 (1969).
[11]D. Schiferl, D. T. Cromer, R. R. Ryan, A. C. Larson, R. LeSar, and L. Robert, Acta Crystallogr., Sect. C **39**, 1151 (1983).
[12]D. T. Cromer, R. L. Mills, D. Schiferl, and L. Schwalbe, Acta Crystallogr., Sect. B **37**, 8 (1981).
[13]G. W. Stinton, I. Loa, L. F. Lundegaard, and M. I. McMahon, J. Chem. Phys. **131**, 104511 (2009).
[14]H. Olijnyk, J. Chem. Phys. **93**, 8968 (1990).
[15]E. Gregoryanz, C. Sanloup, R. Bini, J. Kreutz, H. J. Jodl, M. Somayazulu, H. K. Mao, and R. J. Hemley, J. Chem. Phys. **124**, 116102 (2006).
[16]E. Gregoryanz, A. F. Goncharov, C. Sanloup, M. Somayazulu, H. K. Mao, and R. J. Hemley, J. Chem. Phys. **126**, 184505 (2007).
[17]D. Schiferl, S. Buchsbaum, and R. L. Mills, J. Phys. Chem. **89**, 2324 (1985).
[18]R. Bini, I. Loa, L. Ulivi, J. Kreutz, and H. J. Jodl, J. Chem. Phys. **112**, 8522 (2000).
[19]E. Gregoryanz, A. F. Goncharov, R. J. Hemley, H. K. Mao, M. Somayazulu, and G. Shen, Phys. Rev. B **66**, 224108 (2002).
[20]D. A. Young, C. S. Zha, R. Boehler, J. Yen, M. Nicol, A. S. Zinn, D. Schiferl, S. Kinkead, R. C. Hanson, and D. A. Pinnick, Phys. Rev. B **35**, 5353 (1987).
[21]M. Ross and F. Rogers, Phys. Rev. B **74**, 024103 (2006).
[22]Y. Katayama, T. Mizutani, W. Utsumi, O. Shimomura, M. Yamakata, and K. I. Funakoshi, Nature **403**, 170 (2000).
[23]G. Monaco, S. Falconi, W. A. Crichton, and M. Mezouar, Phys. Rev. Lett. **90**, 255701 (2003).
[24]B. Boates and S. A. Bonev, Phys. Rev. Lett. **102**, 015701 (2009); Phys. Rev. B **83**, 174114 (2011).
[25]G. D. Mukherjee and R. Boehler, Phys. Rev. Lett. **99**, 225701 (2007).
[26]A. F. Goncharov, J. C. Crowhurst, V. V. Struzhkin, and R. J. Hemley, Phys. Rev. Lett. **101**, 095502 (2008).
[27]W. A. Bassett, Rev. Sci. Instrum. **72**, 1270 (2001).
[28]B. J. Baer and C. S. Yoo, Rev. Sci. Instrum. **76**, 013907 (2005).
[29]D. Tomasino and C. S. Yoo, Appl. Phys. Lett. **103**, 061905 (2013).
[30]H. K. Mao, J. Xu, and P. M. Bell, J. Geophys. Res. **91**, 4673, doi:10.1029/JB091iB05p04673 (1986).
[31]Y. Akahama and H. Kawamura, J. Appl. Phys. **100**, 043516 (2006).
[32]R. Boehler, Rev. Geophys. **38**, 221, doi:10.1029/1998RG000053 (2000).
[33]A. P. Jephcoat and S. P. Besedin, Philos. Trans. R. Soc. London, Ser. A **354**, 1333 (1996).
[34]S. Deemyad, A. N. Papathanassiou, and I. F. Silvera, J. Appl. Phys. **105**, 093543 (2009).
[35]R. Boehler, M. Ross, P. Söderlind, and D. B. Boercker, Phys. Rev. Lett. **86**, 5731 (2001).
[36]Z. Jenei, Ph.D. thesis, Stockholm University, 2009, see http://www.dissertations.se/dissertation/e4168ddf51/.
[37]S. Rekhi, L. S. Dubrovinsky, and S. K. Saxena, High Temp. – High Pressures **31**, 299 (1999).
[38]F. Datchi, R. LeToullec, and P. Loubeyre, J. Appl. Phys. **81**, 3333 (1997).
[39]H. Olijnyk and A. P. Jephcoat, Phys. Rev. Lett. **83**, 332 (1999).
[40]V. V. Kechin, Phys. Rev. B **65**, 052102 (2001).
[41]D. Donadio, L. Spanu, I. Duchemin, F. Gygi, and G. Galli, Phys. Rev. B **82**, 020102 (2010).
[42]B. J. Kip and R. J. Meier, Appl. Spectrosc. **44**, 707 (1990).